Biophysical Chemistry 28 (1987) 121–128
Elsevier

BPC 01190

Indefinite isoenthalpic self-association of solute molecules

Ronald C. Chatelier

Section on Pharmacology, Laboratory of Biochemical Pharmacology, National Institute of Diabetes and Digestive and Kidney Diseases, National Institutes of Health, Building 8, Room 222, Bethesda, MD 20892, U.S.A.

Received 21 January 1987
Accepted 29 July 1987

Indefinite self-association; Glutamate dehydrogenase; Statistical thermodynamics; Translational entropy; Rotational entropy; Nonideality

Consideration is given to the indefinite self-association of biological molecules assuming that each step-wise addition of monomer is characterized by the same enthalpy change, and that the second virial coefficients adequately describe the thermodynamic nonideality. Statistical thermodynamic models are used to calculate translational and rotational entropy changes accompanying the addition of each monomer to the aggregate. Three polymerization schemes are explored in which the solute species are modeled as right circular cylinders of various length/radius ratios. The analysis is applied to published data on the self-association of bovine liver glutamate dehydrogenase.

1. Introduction

Certain biological molecules appear to self-associate indefinitely as their concentration is increased. Examples may include purine [1,2], glutamate dehydrogenase [3], lysozyme [4], chymotrypsinogen A [5] and β-lactoglobulin A [6]. Systems exhibiting such behavior are generally analyzed using the (isodesmic) assumption that all step-wise molar association constants are identical. This assumption yields simple analytical expressions which allow facile determination of the 'intrinsic' association constant from a linearized transform of the data. However, statistical thermodynamical calculations of the entropy changes accompanying each step-wise association show that the isodesmic assumption is unreasonable [7]. We therefore present an alternative treatment which employs computation of the translational and rotational entropy changes associated with the addition of each monomer to the aggregate. The calculations require choice of the geometries of all the species, and the association constants obtained from the analysis are therefore dependent on the choice of the polymerization model. Various polymerization schemes are explored in which the solute species are modeled as right circular cylinders. The analysis is applied to the self-association of glutamate dehydrogenase [3].

Correspondence address: R.C. Chatelier, Section on Pharmacology, Laboratory of Biochemical Pharmacology, National Institute of Diabetes and Digestive and Kidney Diseases, National Institutes of Health, Building 8, Room 222, Bethesda, MD 20892, U.S.A.

2. Theory

2.1. Ideal systems

2.1.1. Background thermodynamics

Consider the following set of equilibria which describe the step-wise indefinite self-association of a solute molecule

$$P_{i-1} + P_1 \rightleftharpoons P_i$$

where $i = 2, 3, 4, \ldots$. The system may be described by either weight ($K_{w,i}$) or molar ($K_{c,i}$) equilibrium association constants

$$K_{w,i} = \frac{w_i}{w_1 w_{i-1}} \tag{1}$$

$$K_{c,i} = \frac{c_i}{c_1 c_{i-1}} \tag{2}$$

where w_i and c_i refer to the weight and molar concentrations, respectively, of the i-th species. The two sets of constants are related by the expression

$$K_{w,i} = \frac{i}{M_1(i-1)} \cdot K_{c,i} \tag{3}$$

where M_1 is the molecular weight of monomer.

The weight concentration of each species is related to the weight concentration of monomer by

$$w_i = w_1^i \prod_{j=2}^{i} K_{w,j} \tag{4}$$

Thus the total concentration of solute is

$$w_T = w_1 + \sum_{i=2} w_1^i \prod_{j=2}^{i} K_{w,j} \tag{5}$$

and the weight-average molecular weight of the system is

$$M_w = M_1 \left(\frac{w_1 + \sum_{i=2} i w_1^i \prod_{j=2}^{i} K_{w,j}}{w_T} \right) \tag{6}$$

For computational reasons, it is more convenient to calculate $K_{c,i}/K_{c,2}$ rather than calculating $K_{c,i}$ directly. Assuming that the addition of each monomer to the aggregate is accompanied by the same enthalpy change

$$\ln\left(\frac{K_{c,i}}{K_{c,2}}\right) = \frac{\bar{S}_i - \bar{S}_{i-1} - \bar{S}_2 + \bar{S}_1}{R} \tag{7}$$

where $\bar{S}_i$ is the molar entropy of the i-th species and R the universal gas constant.

2.1.2. Translational and rotational entropies of the solute species

We will assume that the total entropy of a species is given by the sum of the translational and rotational entropies of that species. Various other possible contributions to the term ($\bar{S}_i - \bar{S}_{i-1} - \bar{S}_2 + \bar{S}_1$) are considered in appendix A and shown to be (probably) less important. The molar translational ($\bar{S}_{t,i}$) and rotational ($\bar{S}_{r,i}$) entropies of i-mer are given by [7,8]

$$\bar{S}_{t,i} = R\left(\tfrac{3}{2} \ln iM_1 - \ln c_i + Z_1\right) \tag{8}$$

$$\bar{S}_{r,i} = R\left(\tfrac{1}{2} \ln I_i + Z_2\right) \tag{9}$$

where I_i is the product of the moments of inertia about the three principal axes of the i-mer. The terms Z_1 and Z_2 are functions of a symmetry factor, the temperature, and various fundamental constants (Boltzmann's constant, Planck's constant, and Avogadro's number). Since they are independent of i, Z_1 and Z_2 will disappear upon calculation of $K_{c,i}/K_{c,2}$.

Combining eqs. 7–9 and rearranging

$$\frac{K_{c,i}}{K_{c,2}} = \left[\frac{i}{2(i-1)}\right]^{3/4} \left[\frac{I_i I_1}{I_{i-1} I_2}\right]^{1/4} \tag{10}$$

The evaluation of $K_{c,i}$ requires calculation of the moments of inertia of each species and hence the choice of a shape for each species.

2.1.3. Geometric models of the solute species

The monomers are modeled as right circular cylinders of length l_1 and radius r_1. The product of the moments of inertia about the three principal axes is

$$I_1 = \tfrac{1}{2} m_1 r_1^2 \left(\tfrac{1}{4} m_1 r_1^2 + \tfrac{1}{12} m_1 l_1^2\right)^2 \tag{11}$$

where m_1 is the mass (in g) of the monomer. These monomers are considered to associate according to three hypothetical schemes chosen to encompass a broad range of polymerization mechanisms (fig. 1). Let $\theta = l_1/r_1$ describe the monomer geometry and $\phi_i = l_i r_1 / l_1 r_i$ describe the relationship between the geometries of i-mer and monomer. The product of the moments of inertia of the i-mer about the X, Y and Z axes may be written

$$I_i = m_i^3 r_i^6 \cdot \tfrac{1}{2}\left(\tfrac{1}{4} + \tfrac{1}{12}\theta^2 \phi_i^2\right)^2 \tag{12}$$

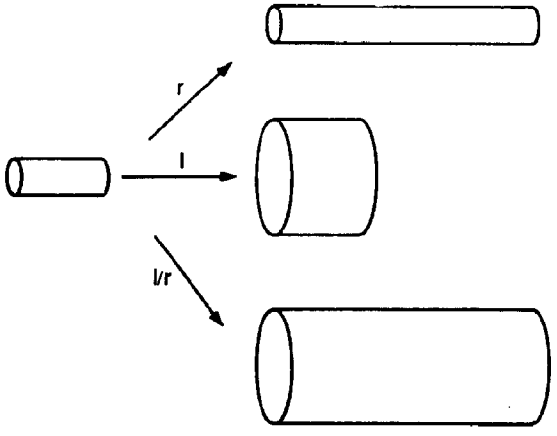

Fig. 1. Schematic representation of right circular cylinders associating such that either the radius, length, or length/radius of the aggregate is identical to that of the monomer.

We further define $\psi_i = m_i^3 r_i^6 / m_1^3 r_1^6$. Thus

$$\frac{I_i I_1}{I_{i-1} I_2} = \frac{J_i J_1}{J_{i-1} J_2} \tag{13}$$

where J_i is related to the reduced terms θ, ϕ_i and ψ_i

$$J_i = \psi_i \left(\tfrac{1}{4} + \tfrac{1}{12}\theta^2 \phi_i^2\right)^2 \tag{14}$$

The expressions for ϕ_i and ψ_i may be further simplified for each of the cases shown in fig. 1.

(a) Conservation of radius: $\phi_i = i$ and $\psi_i = i^3$.

(b) Conservation of length: $\phi_i = i^{-1/2}$ and $\psi_i = i^6$.

(c) Conservation of length/radius: $\phi_i = 1$ and $\psi_i = i^5$.

2.2. Nonideal systems

Nonideality will be treated using two hard-particle models: virial theory and scaled particle theory [9,10]. The osmotic pressure, light scattering, and sedimentation equilibrium behavior of concentrated protein solutions are adequately described by both formalisms [11–14].

2.2.1. Correction of the apparent weight-average molecular weight obtained by sedimentation equilibrium

In nonideal solutions, the apparent weight-average molecular weight ($M_{w,a}$) reported by sedimentation equilibrium is lower than the true weight-average molecular weight (M_w). A semi-empirical correction of $M_{w,a}$ yields M_w to within 10% in a variety of self-associating systems at concentrations up to 400 g/l [14].

Assuming that all species have the same geometry as the monomer, we can calculate a set of three shape factors required by scaled particle theory

$$a = 0.25(\pi + \theta) \tag{15a}$$

$$b = 2\pi(1 + \theta) \tag{15b}$$

$$c = \pi\theta \tag{15c}$$

where $\theta = l_1/r_1$ as in section 2.1.3. A set of apparent virial coefficients derived from scaled particle theory is given by

$$B_i = i\left[1 + \frac{(i-1)(i-2)a^2b^2}{6c^2} + \frac{(i-1)ab}{c}\right] \tag{16}$$

The corrected weight-average molecular weight is obtained from the relationship

$$M_{w,c} = M_{w,a}\left(1 + \sum_{i=2} B_i \phi^{i-1}\right) \tag{17}$$

The volume fraction $\phi = w$ (g/l) v (l/g) where v is the specific volume of the equivalent particle.

2.2.2. Calculation of the apparent equilibrium constants

In nonideal solutions, the apparent step-wise equilibrium constants (K') are related to the true constants by the relation

$$K'_{w,i} = K_{w,i} \frac{\gamma_1 \gamma_{i-1}}{\gamma_i} \tag{18}$$

where γ_i is the activity coefficient of the i-th species. It is difficult to treat indefinite self-association at arbitrary concentration since scaled particle theory may not be used to calculate γ_i when the solute species have different shapes [15], and the virial coefficients B_3-B_7 in a three-dimensional fluid are only available for identical particles [16]. However, a limited treatment of γ_i in terms of the second virial coefficients is possible using the formalism of Kihara [17] as described in appendix B.

3. Results and discussion

Simulated results will be used to demonstrate various features of indefinite isoenthalpic self-association in thermodynamically ideal solutions. Experimental data obtained with glutamate dehydrogenase [3] will then be fitted using the above theory.

Fig. 2A–C shows plots of $K_{c,i}/K_{c,2}$ vs. i for monomers of various length/radius ratios associating according to the three schemes in fig. 1. In all cases, the system is far from 'isodesmic', as has been previously noted [7]. The decrease in equilibrium constant with increasing aggregate size is due to the greater loss of translational and rotational entropy upon association of a monomer with a large aggregate compared to its association with a small aggregate. Values of $K_{c,i}$ become approximately constant at large i because, under these conditions, the entropy of an i-mer is approximately the same as that of an $(i-1)$-mer. When the association is 'end-to-end' (fig. 2A, conservation of radius) an increase in θ results in a decrease in a given equilibrium constant. The opposite trend is observed when the association is 'side-by-side' (fig. 2B, conservation of length). These effects are due to the influence of the moments of inertia of the various species on their rotational entropy, and hence on the values of $K_{c,i}/K_{c,2}$. When all species have the same shape (fig. 2C, conservation of length/radius), the equilibrium constants are insensitive to changes in monomer geometry. This is because when $\phi = 1$, the term $J_i J_1/(J_{i-1}J_2)$ reduces to $i^5/32(i-1)^5$ and is therefore independent of θ.

The indefinite self-association of bovine liver glutamate dehydrogenase [3] will now be considered in the light of the above theory. This system was chosen for discussion because the association is known to be end-to-end [18]. We will assume that the largest aggregate contains 20 monomers, and that the specific volume is the same as the partial specific volume. Data may be fitted according to an indefinite isoenthalpic self-association model in the following way:

(a) For a given polymerization scheme, values of $K_{w,2}$ and θ are chosen. The apparent weight-average molecular weight is corrected for nonideal

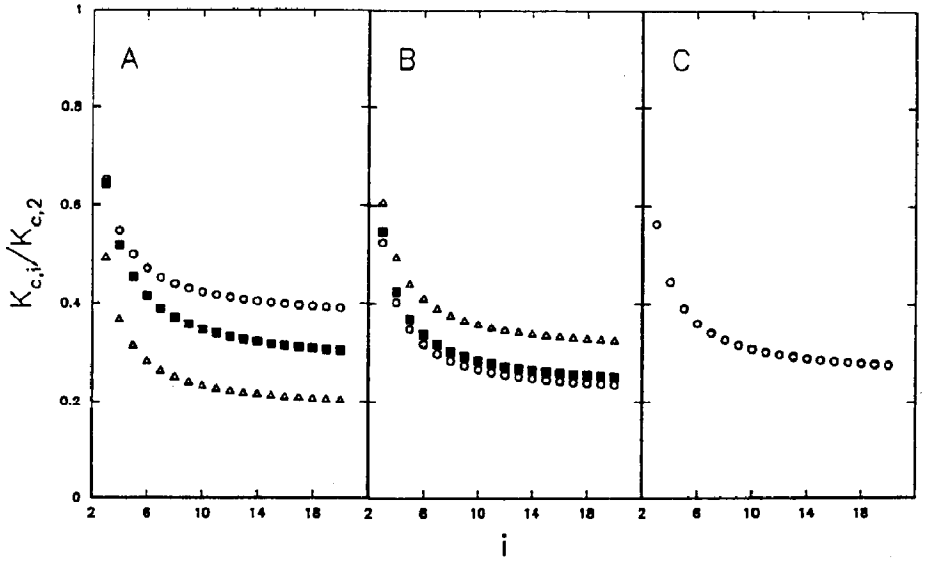

Fig. 2. Plots of $K_{c,i}/K_{c,2}$ vs. i for various polymerization schemes and monomer geometries. (A) Radius of cylinders conserved during aggregation: length/radius of monomer is 0.1 (○), 1 (■), and 10 (△). (B) Length of cylinders conserved during aggregation: length/radius of monomer is 0.1 (○), 1 (■), and 10 (△). (C) Length/radius of cylinders conserved during aggregation.

effects using eq. 17, and the second virial coefficients B_{ij} are calculated using eq. B6. Values of $K_{w,i}$ are computed from eqs. 3 and 10 assuming thermodynamic nonideality, and are corrected for nonideality during the iterative procedure below.

(b) For a given w_T, an initial guess is made of the value of w_1. Initial values of $w_2 - w_{20}$ are calculated using eq. 4.

(c) The γ_i are calculated using eq. B7, and the $K_{w,i}$ are corrected for the effects of nonideality using eq. 18. New values of $w_2 - w_{20}$ are calculated. A better estimate of w_1 is obtained based on a rearrangement of eq. 5

$$w_1' = \frac{w_T}{1 + \sum_{i=2}^{i} w_1^{i-1} \prod_{j=2} K_{w,j}} \qquad (19)$$

Oscillations in the value of w_1 are damped using the relation

$$w_1'' = (w_1' + 2w_1)/3 \qquad (20)$$

(d) Step (c) is invoked repeatedly until the value of w_1 converges. The value of $(M_w/M_1$(experimental) $- M_w/M_1$ (calculated))^2 is then computed.

The shape of the χ^2 surface will be initially explored assuming end-to-end association in a solution which is thermodynamically ideal, and the data will then be fitted to various models which take account of nonideality. Fig. 3 shows a stereo diagram of SSQ vs. $K_{w,2}$ vs. log θ, calculated according to the procedure outlined above. The best-fit value of $K_{w,2}$ is well defined for a given value of θ. However, it is difficult to decide on a best-fit value of θ because the value of SSQ is fairly insensitive to changes in θ. A more detailed examination of the 'valley' in the surface shows that the best-fit value of $K_{w,2}$ is a weakly varying function of θ, with better fits being obtained at lower values of θ (see table 1).

The ability of several models to describe the self-association of glutamate dehydrogenase is explored in detail in table 1. In general, consideration of nonideality resulted in an increase in SSQ for the isodesmic models but a decrease in SSQ for the isoenthalpic models. The isoenthalpic models reported best-fit values of $K_{w,2}$ which were weakly sensitive to the polymerization scheme and the assumed monomer geometry, and were higher than the value obtained from the isodesmic models. Of all the isoenthalpic models considered, the models exhibiting the lowest SSQ coincided with the known behavior of glutamate dehydrogenase, i.e., end-to-end association.

Fig. 4 displays a plot of M_w/M_1 vs. w_T for glutamate dehydrogenase, adapted from fig. 7 of ref. 3, together with a curve generated using the nonideal end-to-end association model and values of $K_{w,2} = 6.6$ l/g and $\theta = 0.5$. The data are approximately described by an isoenthalpic model over this small concentration range. However, the agreement between theory and experiment is not good as shown by the slight but systematic discrepancy between the experimental points and the fitted curve. This discrepancy may arise because

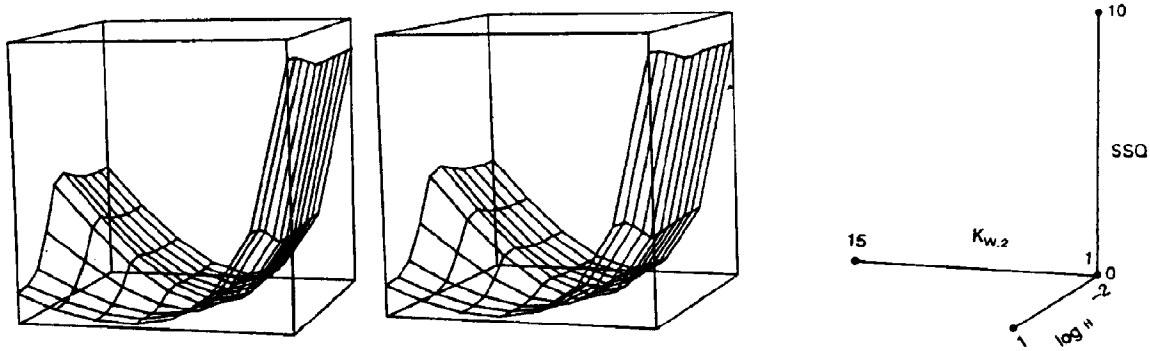

Fig. 3. Stereo diagram of sum of squares of residuals (SSQ) vs. $K_{w,2}$ vs. log θ generated assuming end-to-end association of glutamate dehydrogenase in ideal solution. The data points used in the computation are shown in fig. 4.

Table 1

Best-fit values of $K_{w,2}$ (l/g) for various assumed monomer geometries, polymerization schemes, and association models

Values in parentheses are the sum of squared residuals × 1000.

Polymerization scheme	θ	Isodesmic		Isoenthalpic	
		Ideal	Nonideal	Ideal	Nonideal
Conserve r	0.1	3.8 (44)	3.7 (78)	6.8 (49)	6.7 (36)
	0.3		3.8 (56)	6.6 (43)	6.6 (38)
	0.5		3.8 (52)	6.6 (44)	6.6 (41)
	1		3.8 (49)	7.1 (68)	7.1 (65)
	3		3.8 (47)	8.7 (140)	8.7 (142)
	5		3.8 (47)	9.1 (159)	9.2 (162)
	10		3.9 (45)	9.3 (168)	9.4 (177)
Conserve l	0.1		3.8 (63)	8.7 (137)	8.8 (138)
	0.3		3.8 (53)	8.6 (135)	8.7 (134)
	0.5		3.8 (51)	8.6 (132)	8.6 (131)
	1		3.8 (50)	8.3 (120)	8.3 (118)
	3		3.8 (51)	7.6 (86)	7.6 (83)
	5		3.8 (52)	7.5 (79)	7.4 (75)
	10		3.8 (57)	7.4 (76)	7.4 (70)
Conserve l/r	0.1		3.7 (79)	8.0 (105)	8.0 (92)
	0.3		3.8 (57)		8.0 (99)
	0.5		3.8 (53)		8.0 (101)
	1		3.8 (51)		8.0 (102)
	3		3.8 (51)		8.0 (102)
	5		3.8 (52)		8.0 (101)
	10		3.8 (57)		8.0 (100)

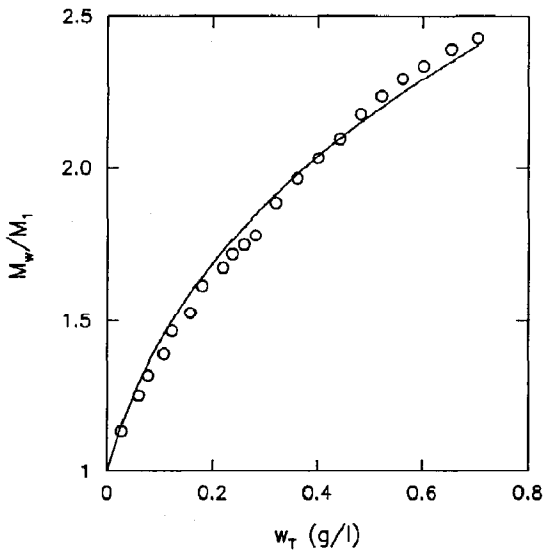

Fig. 4. Plot of M_w/M_1 vs. w_T for the self-association of glutamate dehydrogenase (O) adapted from fig. 7 of ref. 3. The solid line was simulated using isoenthalpic theory pertinent to the case of end-to-end association in nonideal solution with $K_{w,2}$ = 6.6 l/g and length/radius of monomer = 0.5.

the step-wise associations of glutamate are not isoenthalpic, or because the theory is highly oversimplified and approximate. Nevertheless, the isoenthalpic assumption is more reasonable than the isodesmic assumption and further analysis of self-associating systems should therefore proceed by modification of the above germinal theory rather than by reverting back to the isodesmic treatment.

4. Concluding remarks

We have analyzed indefinite self-association taking into account the translational and rotational entropies of the various solute species. Our treatment requires more computation than the previous treatment based on the isodesmic assumption [2]. However, the isoenthalpic assumption is more reasonable and should yield values of the association constants which are closer to the 'true' values. When each monomer can make more than two contacts in the aggregate, it is necessary to refine further the approach and to use approximate methods of counting the average number of contacts as a function of size [19]. Finally, we note that our entropy calculations are only approximate and are based on highly simplified models of the solute species. In particular, the use of straight, smooth cylinders to model the rotational entropies of the solute species may lead to the discrepancy between theory and experiment shown in fig. 4. The results of an analysis based on the above theory should therefore be considered as rough estimates of the step-wise association constants.

Appendix A

In section 2, the aggregates were modeled as rigid bodies. However, real aggregates would be

expected to undergo bending and torsional motions (see fig. 5). Moreover, the association reactions may be accompanied by the release of interfacial water molecules and buffer ions, and may also result in changes in the atomic motions in individual subunits. We therefore explore the affect that such factors may have on the values of $K_{c,i}/K_{c,2}$.

Consider the end-to-end association model, where each monomer is rigid and the i-th monomer may bend through a solid angle α with respect to the axis of the $(i-1)$-th monomer (fig. 5A). Let the entropy of bending of the dimer be

$$\bar{S}_{b,2} = R \ln F(\alpha) \tag{A1}$$

where $F(\alpha)$ is some function of α. Assuming no inter- or intramolecular interactions between subunits in the aggregates, the entropy of bending of the trimer is

$$\bar{S}_{b,3} = R \ln F(\alpha)^2 \tag{A2}$$

since for each configuration of the second subunit, the third subunit is able to bend through a solid angle α. Repeating this argument, one can show that

$$\bar{S}_{b,i} - \bar{S}_{b,i-1} - \bar{S}_{b,2} = 0 \tag{A3}$$

In other words, the bending motions of aggregates per se do not affect the values of $K_{c,i}/K_{c,2}$ as long as the aggregates behave according to the simple bending model shown in fig. 5A. However, a bent rod will not have the same moments of inertia as a straight rod, and bending motions may therefore influence values of $K_{c,i}/K_{c,2}$ via the rotational entropies of the aggregates.

A similar argument holds when the i-th monomer in the aggregate is able to undergo torsional motion about an angle β with respect to the $(i-1)$-th monomer (fig. 5B). Again, these motions do not affect the values of $K_{c,i}/K_{c,2}$.

The association reactions may be accompanied by the release of bound water and buffer ions from the subunit-subunit contact regions. As long as the number of solvent molecules released is independent of aggregate size, this effect will not lead to any changes in $K_{c,i}/K_{c,2}$.

The association of molecules may result in a decrease in atomic motions in the subunit-subunit contact regions. As above, when this effect is independent of aggregate size there will be no alteration in $K_{c,i}/K_{c,2}$.

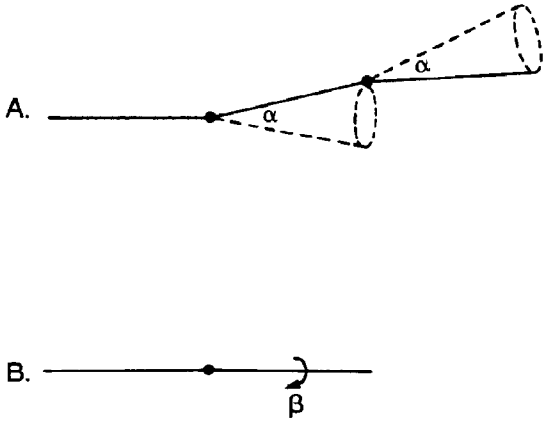

Fig. 5. Schematic diagrams of aggregates showing motions of subunits. (A) Bending about a solid angle α with respect to the axis of a neighboring subunit. (B) Torsional motion about an angle β with respect to a neighboring subunit.

Appendix B

The activity coefficient of an i-mer in a mixture of cylindrical oligomers may be calculated in the following way. Three shape factors for the i-mer are given by

$$a_i = 0.25(\pi + \theta\phi_i) \tag{B1a}$$

$$b_i = 2\pi(1 + \theta\phi_i) \tag{B1b}$$

$$c_i = \pi\theta\phi_i \tag{B1c}$$

The ϕ_i are dependent on the polymerization scheme as outlined in section 2.1.3. A characteristic dimension for the i-mer is

$$R_i \text{ (dm)} = \left(\frac{M_i v}{N_a c_i}\right)^{1/3} \tag{B2}$$

where M_i is the molecular weight of i-mer, v the specific volume of the equivalent particle (1/g), and N_a Avogadro's number. The average radius, and the surface area and volume of the i-mer are

$$\bar{R}_i = a_i R_i \tag{B3}$$

$$S_i = b_i R_i^2 \tag{B4}$$

$$V_i = c_i R_i^3 \tag{B5}$$

The molar excluded volume of any two convex particles is [17]

$$B_{ij} = N_a\left(V_i + V_j + \bar{R}_i S_j + \bar{R}_j S_i\right) \tag{B6}$$

where i and j represent the solutes. The activity coefficient of the i-th species is then given by

$$\gamma_i = \exp\left(\sum_{j=1} B_{ij} c_j\right) \tag{B7}$$

where c_j is the molar concentration of the i-th species. We note that this treatment is only valid when three-body interactions do not contribute substantially to the nonideality.

Acknowledgments

I am grateful to Dr. Allen P. Minton for his support and help during the course of this work, and for reviewing the initial draft of this manuscript. I would also like to thank Dr. Terrell L. Hill for helpful discussions.

References

1 S.I. Chan, M.P. Schweizer, P.O.P. Ts'o and G.K. Helmkamp, J. Am. Chem. Soc. 86 (1964) 4182.
2 K.E. Van Holde and G.P. Rossetti, Biochemistry 6 (1967) 2189.
3 E. Reisler, J. Pouyet and H. Eisenberg, Biochemistry 9 (1970) 3095.
4 P.R. Wills, L.W. Nichol and R.J. Siezen, Biophys. Chem. 11 (1980) 71.
5 D. Hancock and J.W. Williams, Biochemistry 8 (1969) 2598.
6 E.T. Adams, Jr. and M.S. Lewis, Biochemistry 7 (1968) 1044.
7 T.L. Hill and Y.-D. Chen, Biopolymers 12 (1973) 1285.
8 W.J. Moore, Physical chemistry, 3rd edn. (Prentice-Hall, Englewood Cliffs, NJ, 1962) ch. 15.
9 J.L. Lebowitz, E. Helfand and E. Praestgaard, J. Chem. Phys. 43 (1965) 774.
10 R.M. Gibbons, Mol. Phys. 17 (1969) 81.
11 P.D. Ross and A.P. Minton, J. Mol. Biol. 112 (1977) 437.
12 A.P. Minton, Mol. Cell. Biochem. 55 (1983) 119.
13 A.P. Minton and H. Edelhoch, Biopolymers 21 (1982) 451.
14 R.C. Chatelier and A.P. Minton, Biopolymers 26 (1987) 507.
15 R.M. Gibbons, Mol. Phys. 18 (1970) 809.
16 F.H. Ree and W.G. Hoover, J. Chem. Phys. 46 (1967) 4181.
17 T. Kihara, Rev. Mod. Phys. 25 (1953) 831.
18 H. Eisenberg and E. Reisler, Biopolymers 9 (1970) 113.
19 F.A. Ferrone, J. Hofrichter and W.A. Eaton, J. Mol. Biol. 183 (1985) 611.